

Design and manufacture of face grinding wheels with micro-structured channels

Lukas Steinhoff¹, Emma Tubbe¹, Folke Dencker¹, Tim Denmark², Lars Kausch², Marc Christopher Wurz¹

¹Institute of Micro Production Technology (IMPT), Garbsen, Germany

²Schmitz Schleifmittelwerk GmbH, Remscheid, Germany

steinhoff@impt.uni-hannover.de

Abstract

In this study, we demonstrate the design and manufacture of face grinding wheels with micro-structured fluid channels for the uniform distribution of cooling lubricant in the tool working zone. For this purpose, the effect of different channel geometries on the flow velocity and the pressure exerted by the fluid on the channel wall is tested simulatively. To ensure effective heat exchange between the coolant and the workpiece, the channel geometry was designed to achieve a large contact area between the fluid and the ground material. Here, the tested curved channel geometries showed to have about 5 % more area than straight channels. However, the higher influence here is exerted by the number of channels. The produced curved channels further showed a direct influence on the flow rate of the cooling lubricant depending on the direction of rotation of the grinding wheel. This allows slowing down the flow rate by 2 % or increase it by up to 18 % compared to straight channels. We observed a beneficial influence to the flow rate and thus also the heat exchange without changing the pump parameters of the fluid. Prototype grinding wheels were produced by microsystem technology. For this purpose, silicon carbide is mixed as an abrasive into a photosensitive polymer (flexible binding matrix) and applied to a steel substrate. Structuring takes place by using photolithography. The unexposed areas can be cleared using developer solution. These form the channel structures. The cooling lubricant, for which water was selected, is supplied via the spindle and thus via the tools centre. The achievable minimum channel width is 200 μm or greater with a depth of 50-60 μm . First grinding tests resulted in roughness values of $R_a = 0.07 \pm 0.03 \mu\text{m}$ and $R_z = 3.38 \pm 1.96 \mu\text{m}$ for dry machining and $R_a = 0.08 \pm 0.03 \mu\text{m}$ and $R_z = 1.92 \pm 0.20 \mu\text{m}$ for machining with water as cooling lubricant. Temperature measurements proofed that the temperature increase of around $8 \cdot 10^{-4} \text{ }^\circ\text{C/s}$ could be decreased to around $2 \cdot 10^{-4} \text{ }^\circ\text{C/s}$ by use of water als cooling lubricant.

Keywords: micro grinding, micro production technology, precision engineering, lubricant distribution

1. Introduction

Grinding as a mechanical machining process is an important step in achieving the required surface quality as well as dimensional accuracy of a component and is often used as finishing process in different fields, like automobile or aerospace [1]. However, the process harbours challenges that can prevent the required surface quality. Grinding burn is one of them [2]. Excessively high temperatures in the grinding zone can lead to damage to the material surface e.g. high residual stresses. A reduction in friction and reduction of the generated heat can be achieved through the application oriented use of cooling lubricants (CL) [3]. The reduction in temperature can be maximised by guiding the CL through the tool directly into the contact zone between tool and workpiece. This continues to be an issue in the field of toolmaking and the associated research. Therefore, there are already some approaches to solving the problem. One group constructed a peripheral grinding wheel from a sandwich system consisting of several layers into which channels for the distribution of CL were inserted [4]. Another approach shows a face grinding wheel with an interrupted abrasive layer and guided cooling lubricant feed via the spindle [5].

This paper presents the process of manufacturing a grinding wheel for achieving high surface qualities with a structured grinding layer using photolithography. For this purpose, a polyimide with embedded abrasive grains (silicon carbide, SiC) is used as a binding matrix, which has already been shown as a

suitable combination for production of micro grinding tools [6]. Sufficient CL distribution should be achieved by creating fluid channels in the grinding layer, through which the CL can flow from the centre of the tool. Hereby, photolithography offers the advantage of variable channel geometry. After production, initial grinding tests should demonstrate the functionality of the tools.

2. Experimental procedures

The following section describes the simulation based design of the grinding wheel, the manufacturing process and its structuring by photolithography as well as the first grinding experiments.

2.1. Simulation-based design of the grinding wheel geometry

The aim of this research is to design and manufacture a face grinding wheel with a size of 100 mm, which should feature photolithographically structured fluid channels. The channel width should be in the range of a few hundred micrometres, while the channel depth should correspond to the grinding layer height. Various geometries were therefore created as 3D models using *SolidWorks*. Straight and curved channels as well as angular and radius channel transitions are tested. The pressure distribution on the channel walls through the CL during rotation of the grinding wheel was simulated using *Ansys Fluent*. The pressure distribution serves as a decision criterion here. The aim is to achieve the smoothest possible transition with homogeneous pressure distribution, to minimise the risk of the

abrasive layer detaching from the substrate due to excessive pressure peaks. A rotational speed of 4,000 rpm and a mass flow of 0.0004 kg/s were defined as parameters, as these could become possible grinding parameters for the tool. The pressure distribution on the channel wall and the velocity distribution of the fluid within the channel were extracted as a result of the simulation.

2.2. Manufacturing and characterisation process of micro-grinding tools

Micro-technical structuring using photolithography was chosen for the production of the grinding discs. This allows various geometries and customisations to be realised. The abrasive layer is produced from the photosensitive polyimide LTC9320 (Fujifilm) and SiC abrasive grains (grain size distribution 4-6 μm). Both components are mixed in a glass container to form a homogeneous polyimide abrasive solution (PAS) (Fig. 1a). Steel wafers (1.4301) with a diameter of 100 mm are used as a substrate to produce the grinding tools. The PAS is applied to this by means of spin coating. After a two-part softbake (70 $^{\circ}\text{C}$ for 10 min, 100 $^{\circ}\text{C}$ for 10 min), the grinding wheels are slowly cooled to room temperature. The PAS is then exposed for 250 s using a glass mask to produce the channel geometries. Subsequent development takes place in a 3-stage immersion bath in cyclopentanone, propylene glycol methyl ether acetate (PGMEA) and isopropanol (Fig. 1b). In total, the process from mixing to developing, including handling, takes around two hours. Finally, the grinding wheels cleaned with DI water are baked in an N_2 gas atmosphere at 350 $^{\circ}\text{C}$ for 60 min. The fluid channels are analysed for residues of PAS using light microscopy and the layer thickness is measured using tactile profilometry. In a post-processing step, a 4 mm hole is drilled in the centre of the grinding wheel for the CL connection (Fig. 1c).

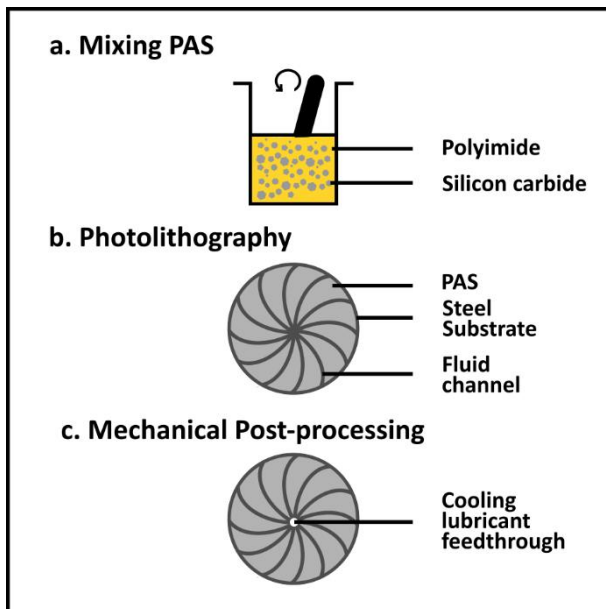


Figure 1. Schematic of the manufacturing process. It is divided in the mixing process of the PAS (a.), the structuring of the fluid channels by photolithography (b.) and the mechanical post-processing (c.).

2.3. Grinding experiments with temperature measurement

In order to ensure a supply of CL through the grinding wheel for the grinding tests, a test setup was designed. The schematic cross-section and a photo of the setup are shown in Fig. 2. The grinding wheel is attached to the grinding wheel mounting using adhesive film. The mounting offers nine places on top for the placement of weights in order to set a defined contact pressure

of approximately 625 Pa and 1,250 Pa for the experiments. The CL is supplied via a tube that is connected to the grinding wheel via a swivel joint. The tube is also hung in a reservoir of the used CL, which is supplied by a peristaltic pump. Mass flow rates of 150 ml/min and 300 ml/min were selected. The grinding wheel is driven by a toothed belt, which is moved by a DC motor. A rotation speed of 80 rpm has been set for the grinding wheel as working speed, which is limited by the motor. As CL water is chosen, whereas dry machining is chosen as comparison.

Stainless steel with a diameter of 130 mm was chosen as the material to be machined. In order to make a statement about the resulting temperatures and the cooling capacity of the cooling medium, temperature sensors of type Pt1000 were attached to the rear of the workpiece in milled pockets with a distance of 300 μm to the front side (see Fig. 2a). A total of three sensors were attached, each at a distance of 20 mm, 30 mm and 40 mm from the centre. This array allows an in situ monitoring of the temperature homogeneity. The measurement data was recorded continuously for 10 min during grinding using a QuantumX measurement amplifier from HBM. Ten measured values were recorded per second. In order to make a statement about the cooling performance, the gradients of the temperature curves were compared with each other. Furthermore, images of the ground surface were taken using confocal laser scanning microscopy in order to assess the surface roughness values R_a and R_z and therefore the grinding performance of the tools. Surface roughness values were obtained over an area of 200 x 200 μm^2 .

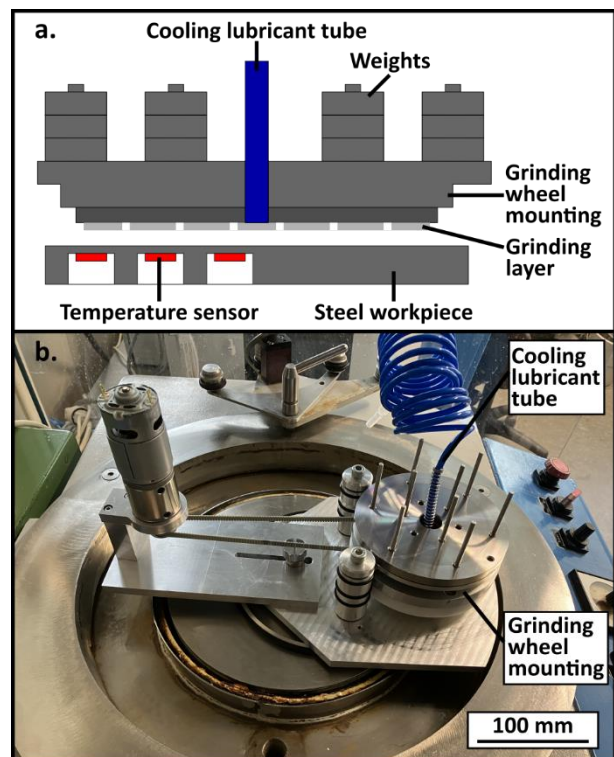


Figure 2. Illustration of the experimental setup for carrying out grinding tests with temperature measurement. A schematic cross-section with the position of the temperature sensors (a.) and a real image of the assembled test stand (b.) are shown.

3. Results and discussion

3.1. Design and manufacturing

In the simulation, the first aim was to investigate two different transitions between the connection of the grinding wheel to the cooling lubricant feed line and the microstructured cooling

channels. As shown in Fig. 3, an angular transition (Fig. 3a) and a radius transition (Fig. 3b) are compared. A normalised pressure decrease distribution is shown. The radius transition shows a much more homogenous and in total lower pressure decrease. Here, the pressure drops very evenly over a longer distance than with the angular transition. In this case, there is a concentrated load directly at the transition, which could lead in the worst case to delamination of the grinding layer.

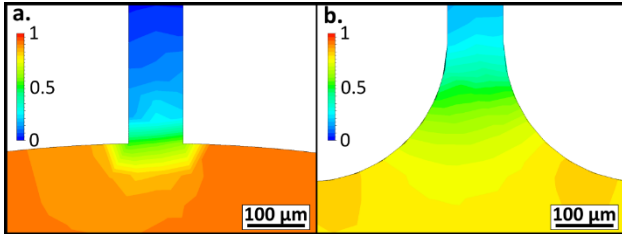


Figure 3. Illustration of the simulation results for comparing an angular transition (a.) and a radius transition (b.). The normalised pressure distribution from the fluid to the solid materials is shown.

Furthermore, straight channels were compared with curved ones. The flow velocity within the channels is used as comparison. The aim is to achieve a high flow velocity for a constant supply of fresh CL. Both types showed an increase in speed from the beginning to the end of the channel. However, the curved channels showed a dependence on the direction of rotation. If the curves of the channel are the opposite direction to the direction of rotation of the tool, the speed is decreased by about 2 % in comparison with straight channels. In numbers it is 21.3 m/s at the end of straight channels and for curved channels around 20.9 m/s. If the rotation direction is in the same direction, an acceleration can be detected by around 18 % (25.1 m/s). This has the advantage that more fresh CL is fed over the grinding zone, resulting in a greater temperature gradient between the workpiece and CL. Another, bigger advantage of the curved channels is the contact surface between the fluid and the workpiece. Due to the channel layout, this is about 5 % larger with curved channels (5.1 mm²) than with straight ones (4.9 mm²), which results in more surface area for heat exchange. This is further increased with the number of channels, which applies for both geometries. Based on these results, the design of the first grinding wheels with radius transitions and 36 curved channels is created.

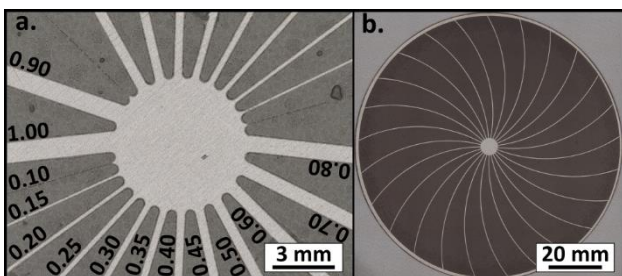


Figure 4. Illustration of the photolithographically structured grinding wheels. The results of a test on the feasible channel width are shown on the left (a.). Above the channels, the channel width from 0.10 mm to 1.00 mm is marked. A grinding wheel with a channel width of 300 µm is shown on the right (b.).

The channel width was evaluated in a feasibility experiment. The aim was to find a compromise between small channels with good manufacturability. The results are shown in Fig. 4. The smallest channels with a width of 100 and 150 µm still showed residual material within the channel structures even after a

longer development time with simultaneous ultrasonic support while at some points over development could already be detected. The 200 µm wide structures could be developed well (Fig. 4a). With regard to the later transfer to larger grinding wheels with thicker grinding layers, a slightly larger channel geometry was chosen. The channel width was therefore set to 300 µm. The first face grinding wheels with the set parameters were then produced with a layer thickness of approx. 50 µm (Fig. 4b).

3.2. Grinding experiments

The grinding wheels produced and shown in Fig. 4b were then used in grinding tests in the setup shown in Fig. 2. The recorded temperature curves were analysed and the resulting temperatures were evaluated for the different CL used. A comparison between dry machining (red) and machining with water as CL (blue) is shown in the following Fig. 5 for the outermost sensor. The range in which the temperature gradient was calculated is also shown as an example.

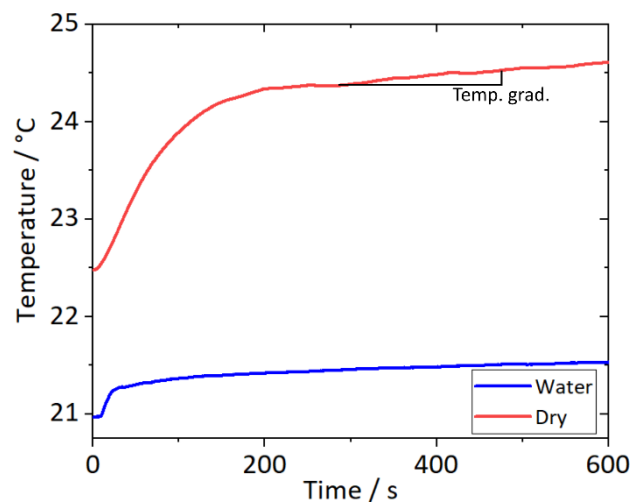


Figure 5. Exemplary evaluation of the recorded temperature during a grinding test. Both curves were recorded by the outermost sensor (40 mm). The tests were carried out at a contact pressure of 1,250 Pa. The CL feed rate was 150 ml/min. The determined temperature gradient for the subsequent comparison of the individual grinding tests is shown.

The temperature development in the first few seconds is significantly higher in most tests, as this is when the workpiece has the highest roughness, the lubricant has not yet been fully distributed and the tool is conditioned in the first few seconds. The abrasive grains can be covered with bond matrix after the manufacturing process, which is why the cutting effect is low but the friction is higher. As soon as the bonding matrix has reset and the abrasive grains can penetrate the workpiece with their cutting edges, the friction is reduced. Furthermore, the absolute initial temperature is not comparable, as this is related to the laboratory conditions and the cooling time of the workpiece between the individual grinding tests. The temperature gradient was therefore selected as the comparison factor. In all tests, an approximately linear curve was obtained after the initial time. It could be observed that the gradient depends on whether CL is used or not. The results are listed in Fig. 6 below. The gradients are small in both cases. This is partly due to the position of the temperature sensors, as the heat must first be conducted through the residual material to the sensor surface and part of it is already dissipated via the remaining workpiece. Furthermore, the rotational speeds and contact pressures are low due to the test setup. Nevertheless, a difference can be observed between dry machining and the use of CL. In dry

machining, the values are approx. 3 times higher than in wet processing with water. It can also be seen that the temperature rises more in the outer machining area than in the inner area. In the case of dry machining, the temperature gradients from sensor to sensor (inside to outside) are each 10 % higher. As both the workpiece and the tool are not moved in a plane, the cutting speed increases due to the increasing radius at a constant speed, resulting in more mechanical interaction. The higher layer thickness results in a higher contact pressure in specific area with the same effective weight. A significant difference between the selected CL quantities could not be determined. However, the resulting absolute temperatures are still very low. At higher cutting speeds and higher contact pressures and thus higher temperatures, the use of cooling lubricant and in particular the quantity will play a greater role than with the process parameters selected in this study.

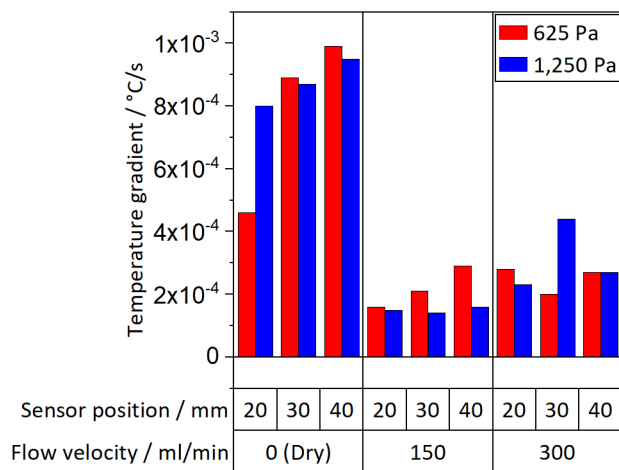


Figure 6. Illustration of the temperature gradients from the grinding tests as a function of the selected cooling lubricant and the grinding parameters used. Red represents the used contact pressure of 625 Pa and blue the used contact pressure of 1,250 Pa.

Fig. 7 shows a comparison of the workpiece surface before and after dry machining for 10 min. For the most part, homogeneous grinding marks can be seen on the machined surface and less heterogeneously distributed scratch marks than on the unmachined surface.

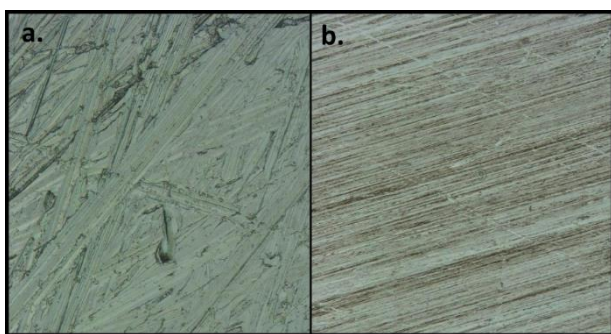


Figure 7. Comparison of the workpiece surface before grinding (a) and after 10 min dry grinding (b).

This is also reflected in the roughness values. Before grinding, the roughness values were $R_a = 0.29 \pm 0.08 \mu\text{m}$ and $R_z = 5.37 \pm 0.91 \mu\text{m}$, which then decreased after machining to $R_a = 0.07 \pm 0.03 \mu\text{m}$ and $R_z = 3.38 \pm 1.96 \mu\text{m}$. With regard to the surface roughness achieved, 10 min machining with water lead to roughness values of $R_a = 0.08 \pm 0.03 \mu\text{m}$ and $R_z = 1.92 \pm 0.20 \mu\text{m}$.

4. Conclusion

In this work, a process for the manufacturing of grinding wheels using microsystems technology with a photolithographically structured grinding layer was demonstrated. The design was created by testing different geometries in a simulation, making it possible to demonstrate the effects of changes in geometry. A radius transition of the CL inlet led to a more homogeneous pressure distribution compared to an angular transition. Furthermore, curved channel structures showed the advantages of reduced flow velocity (-2 %) and a larger contact surface (+5 %) with the workpiece compared to straight channels. After the first design evaluation, a further check by means of finer geometry modifications, like radius of the curved channel or the channel transitions, can be useful for optimization. A test of the possible minimum channel width showed that channels with a width of 200 μm or greater can be produced using microsystem technology with SiC as abrasive grains and polyimide as binding matrix. In the first grinding tests, it was shown by measuring the resulting temperature that the temperature increase during dry machining is approx. 3 times higher than when machining with water as CL. In dry machining, an increase in surface quality to roughness values of $R_a = 0.07 \pm 0.03 \mu\text{m}$ and $R_z = 3.38 \pm 1.96 \mu\text{m}$ was achieved. After wet machining surface roughness values of $R_a = 0.08 \pm 0.03 \mu\text{m}$ and $R_z = 1.92 \pm 0.20 \mu\text{m}$ could be measured. The first grinding tests with the manufactured grinding wheels were therefore already successful. Further investigations into tool wear and optimised machining strategy and machining parameters must now follow in order to determine the performance of the grinding wheels. Other CL are also to be investigated and compared with the previous water cooling system. Furthermore, other structuring methods such as moulding or stamping processes for structuring are to be tested.

Acknowledgement

The authors would like to thank the Federal Ministry for Economic Affairs and Climate Action (BMWK) for their organizational and financial support within the project "PolyGrind" (KK5226203EB1, KK5354801EB1).

References

- [1] Kishore K, Sinha M K, Singh A, Archana, Gupta M K, Korkmaz M E 2023 A comprehensive review on the grinding process: Advancements, applications and challenges *J Mechanical Engineering Science* **236** 10923-10952
- [2] Irani R A, Bauer R J and Warkentin A 2005 A review of cutting fluid application in the grinding process *Int. J. Mach. Tool. Manu.* **45** 1696-1705
- [3] Yang K Z, Pramanik A, Basak A K, Dong Y, Prakash C, Shankar S, Dixit S, Kumar K, Vatin N I 2023 Application of coolants during tool-based machining – A review *Ain Shams Eng. J.* **14** 101830
- [4] Nadolny K 2015 Small-dimensional sandwich grinding wheels with a centrifugal coolant provision system for traverse internal cylindrical grinding of steel 100Cr6 *Journal of Cleaner Production* **93** 354-363
- [5] Peng R, Huang X, Tan X, Chen R, Hu Y 2018 Performance of a pressurized internal-cooling slotted grinding wheel system *Int J Adv Manuf Technol* **94** 2239-2254
- [6] Steinhoff L, Ottermann R, Dencker F, Wurz M C 2023 Detailed characterisation of batch-manufactured flexible micro-grinding tools for electrochemical assisted grinding of copper surfaces *Int. J. Adv. Manufact. Technol.* **128** 2301-2310